AIP | Applied Physics Letters

Partially filled electrodes for digital microfluidic devices

D. G. Pyne, W. M. Salman, M. Abdelgawad, and Y. Sun

Citation: Appl. Phys. Lett. **103**, 024103 (2013); doi: 10.1063/1.4813260
View online: http://dx.doi.org/10.1063/1.4813260
View Table of Contents: http://apl.aip.org/resource/1/APPLAB/v103/i2
Published by the AIP Publishing LLC.

Partially filled electrodes for digital microfluidic devices

D. G. Pyne,[1] W. M. Salman,[2] M. Abdelgawad,[2,a)] and Y. Sun[1,a)]
[1]Department of Mechanical and Industrial Engineering, University of Toronto, Toronto M5S 3G8, Canada
[2]Department of Mechanical Engineering, Assiut University, Assiut 71515, Egypt

(Received 24 May 2013; accepted 20 June 2013; published online 10 July 2013)

As digital microfluidics technology evolves, the need for integrating additional elements (e.g., sensing/detection and heating elements) on the electrode increases. Consequently, electrode area for droplet actuation is reduced to create space for accommodating these additional elements, which undesirably affects force generation. Electrodes cannot simply be scaled larger to compensate for this loss of force, as this would also increase droplet volume and thereby compromise the advantages thought in miniaturization. Here, we present a study evaluating, numerically with preliminary experimental verification, different partially filled electrode designs and suggesting designs that combine high actuation forces with a large reduction in electrode area. © *2013 AIP Publishing LLC*. [http://dx.doi.org/10.1063/1.4813260]

Digital microfluidic devices, as a platform technology, enable programmed manipulation of small droplets on arrays of microelectrodes[1,2] for performing tasks such as polymerase chain reaction (PCR), cell culture, and immunoassays.[3–5] In digital microfluidic devices, conductive or polar droplets are moved under the effect of electrodynamic forces. These forces are generated by the electric field induced from the energized electrode beneath the droplet.[6]

To increase capabilities of digital microfluidic devices, researchers have begun integrating additional elements within electrodes such as impedance spectroscopy,[7] electrophoresis electrodes for particle separation,[8] absorbance detection windows,[9] heaters,[10] field effect transistor-based biosensors,[11] and cell culture patches.[3] As these elements are added, electrode area for droplet actuation is reduced, and force generation becomes weaker. Electrodes cannot simply be scaled larger to compensate for this lower actuation force since this would also increase the droplet volume thereby compromising miniaturizing advantages and increasing device foot print. Therefore, understanding the effect of reducing electrode area on generated forces and droplet speed is necessary.

Here, we present a detailed study evaluating different partially filled electrode designs and suggesting designs that combine a high actuation force with a large reduction in electrode area that permits integration of large elements within the electrode. As a sample application, we present a non-ITO (indium tin oxide), partially filled Cr electrode design that permits the imaging of droplet contents using standard transmission microscopy.

Devices tested in this study were fabricated in the cleanroom facilities at the University of Toronto Nanofabrication Center. Precoated chromium glass slides (Deposition Research Labs Inc., St. Charles, MO), were first primed with Hexamethyldisilazane (HMDS) before spin coating Shipley S1811 photoresist (3000 rpm, 30s). Substrates were then baked to remove solvents (115 °C, 2 min), and UV exposed through a transparency mask (8s). Substrates were next developed in MF-321 (2 min), hard baked (115 °C, 1 min), etched with Chromium etchant CR-4 (2 min) and photoresist removed with AZ-300T stripper (15 min in ultrasonic bath). A 2 μm thick dielectric layer of Parylene C was then deposited by vapor deposition. Lastly, a hydrophobic coating of Teflon AF was spin coated on the device (2000 rpm, 1 min), and baked (160 °C, 10 min). Different designs of partially filled electrodes, Fig. 1, were patterned in chromium to be tested in droplet actuation. A second glass slide, coated with un-patterned ITO (Deposition Research Labs Inc., St. Charles, MO) and Teflon AF, was used as the ground electrode, and the droplet was actuated in between these two glass slides which were separated by a 140 μm spacer (2 pieces of double sided tape).

To quantify the effect of removing electrode area, actuation forces on different designs of partially filled electrodes were simulated using finite element analysis (COMSOL MULTIPHYSICS). Relevant dimensions used in simulation are

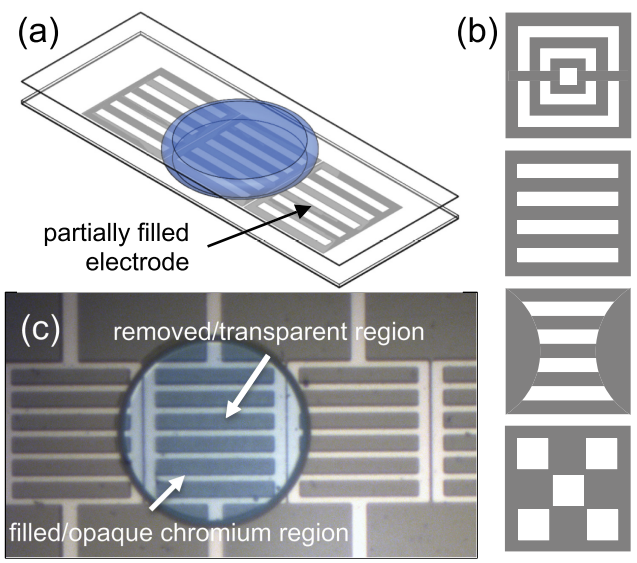

FIG. 1. (a) Schematic of partially filled electrodes providing space for additional on-chip tools or as a window for imaging. (b) Example designs of partially filled electrode configurations considered. Electrodes are 1 mm × 1 mm (c) Image of droplet on series of partially filled electrodes.

a)Authors to whom correspondence should be addressed. Electronic addresses: mohamed.abdelgawad1@eng.au.edu.eg and sun@mie.utoronto.ca

TABLE I. Parameters used in numerical simulation.

Parameter	Value
Electrode dimensions	$1 \times 1\,\text{mm}^2$
Dielectric thickness	$10\,\mu\text{m}$
Droplet radius	$740\,\mu\text{m}$
Droplet contact radius	$600\,\mu\text{m}$
Droplet height	$140\,\mu\text{m}$
Droplet conductivity (σ)	5.5×10^{-6} S/m
Relative permittivity of droplet	80
Relative permittivity of air	1
Relative permittivity of dielectric	2.5
Actuation voltage	100 V

summarized in Table I. Droplet was modelled as a non-deformable lossy dielectric and hence, the conservation of charge [Eq. (1)] and Laplace [Eq. (2)] applies[12]

$$\nabla(\sigma \nabla V) = 0, \tag{1}$$

$$\nabla(\varepsilon \nabla V) = 0, \tag{2}$$

where $\varepsilon = \varepsilon_r \varepsilon_0$ (ε_r is the relative permittivity of the medium, and ε_0 is the permittivity of free space), σ is the electrical conductivity of the droplet, and V is the electric potential. Actuation forces are then calculated by integrating the Maxwell stress tensor over the surface of the droplet, assuming negligible magnetic fields,[13] according to

$$\mathbf{F} = \int_S \mathbf{T} \cdot \mathbf{n} ds, \tag{3}$$

$$\mathbf{T}_{ij} = \varepsilon(E_i E_j - 0.5\,\delta_{ij} E^2), \tag{4}$$

where $\mathbf{T}_{ij}$ is the Maxwell stress tensor. Actuation forces were calculated over a series of droplet locations along its actuation path. Since the integration of the Maxwell stress tensor is dependent on mesh geometry and density, a uniform swept mesh is used to allow for a fine mesh on the droplet leading and trailing faces without considerably increasing the total number of elements, Fig. 2(a). Swept layers are distributed in the vertical direction following a geometric sequence so that layers are denser near the underlying dielectric layer to avoid a large jump in element size at the droplet and dielectric interface.

Fig. 2(b) shows force curves as a function of droplet position. This approach enables quantifying the quality of any arbitrary electrode design. Forces on the leading surface of the droplet are dominant except at the end of droplet motion when the trailing surface produces a reverse force on the droplet, which leads to droplet motion stopping on the center of the electrode. Position is defined as the distance from the left edge of the electrode to the leading edge of the droplet.

The goal of simulations was to address two questions in the design of partially filled electrodes: how the removed electrode area affects actuation forces and where electrode removal is most critical to force generation. To answer the first question, a horizontally striped electrode design with variable strip width was simulated, and the relationship between electrodynamic force and electrode fill percentage was determined [Fig. 2(c)]. Force was found to have a linear relationship with fill percentage, which is expected as the majority of force is generated at the advancing three phase contact line of the droplet. In these simulations, the length of the contact

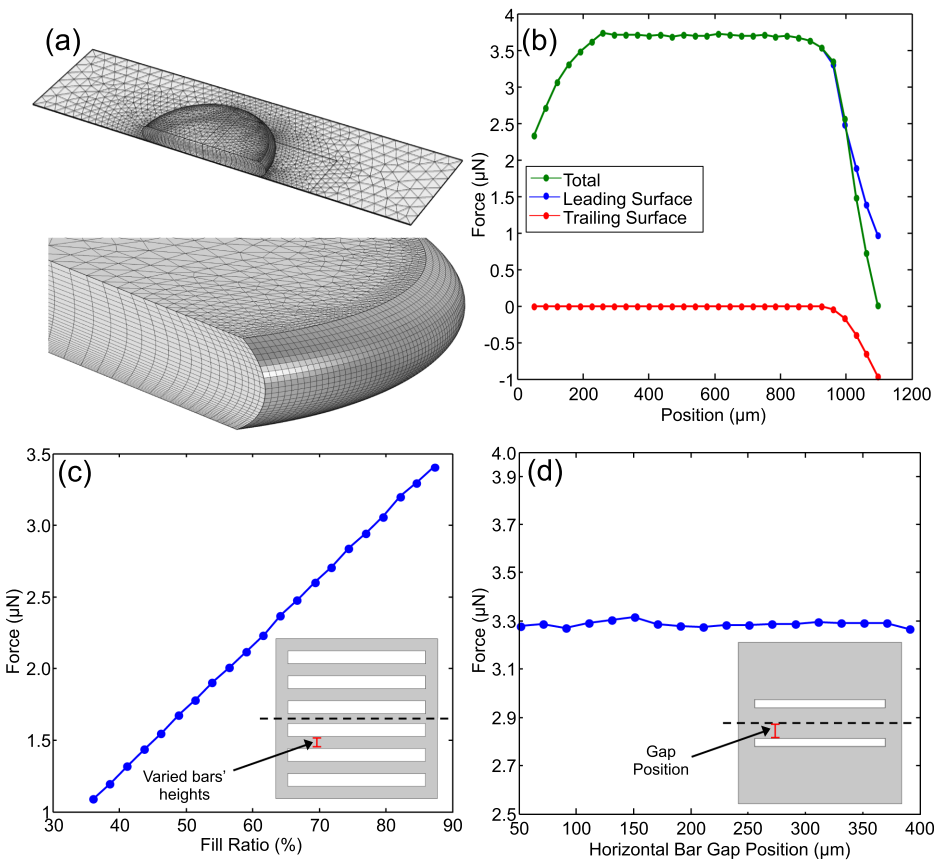

FIG. 2. Simulation results. (a) Droplet half space mesh and swept uniform mesh on droplet surfaces. (b) Actuation force on droplet for conventional electrode on leading and trailing droplet surfaces. Reverse actuation force is generated on trailing droplet surface as backward interface begins to move onto electrode. (c) Induced forces increase linearly with electrode fill ratio, which was changed by varying the width of the horizontal bars in the electrode. (d) Force is independent of vertical location of removed area from electrode. The leading edge of the droplet is fixed at the midpoint of the electrode for panels (c) and (d).

line in contact with the electrode increases approximately linearly as the fill percentage is increased (i.e., as the horizontal strips are widened), which leads to the linear increase in force.

To answer the second question of assessing the location effect of electrode area removal on the induced force, an electrode with a single horizontal window was studied. The distance between the window and the centerline of the electrode was then varied to test the position dependence in the perpendicular axis [Fig. 2(d)]. Vertical position of the removed portion of the electrode was found to have no effect on force generation. Since most of the actuation force is generated on the contact line, this result can be explained by considering the amount of force lost in the horizontal window. As the window moves farther from the centerline and the contact line curves, a larger length of it is placed inside the window. However, the generated force per length is normal to the droplet surface; therefore, the component of the actuation force parallel to the centerline is proportional to the vertical projection of the contact length. Since this projection remains constant as the window moves away from the centerline, there is no force dependence on the position of the removed portion. These results lead to the conclusion that force generation is dominated by total electrode area and at any particular position, by the vertical projection of the three phase contact line in contact with the filled area of the electrode.

In addition to its effect on the generated force on the droplet, filled areas of the electrode should be distributed in a manner that does not compromise the initial pulling force at the beginning of the motion where generated forces are at its lowest. This is critical to produce a large enough force to induce motion and overcome line pinning. Large initial pulling forces can be achieved by making sure that the entrance area of the electrode is always completely filled as a crescent that matches the droplet's leading edge, as shown in Fig. 3(a). Removal of a portion of the electrode, in the form of horizontal stripes or any other form, can then follow to allow for the integration of various elements into the electrode. This shape guarantees that maximum force is applied to the advancing contact line at the crucial stage of initiating droplet motion. This filled crescent is mirrored at the other side of the electrode to provide strong droplet motion in both directions, but it can be removed if droplet motion is desired only in one direction allowing for an even larger area for the integration of other device elements.

To experimentally evaluate the effect of reducing the energized electrode area, we compared the maximum droplet actuation frequency (i.e., how many electrodes can the droplet cross per second) on partially filled and solid electrodes. Droplet motion was controlled using a custom LabVIEW program controlling an array of 24 relays connected to a high voltage amplifier (Trek PZD350A, Medina NY). Motion was then recorded using a CCD camera (Basler acA1300-30gc, Exton PA) connected to a motorized zoom lens (Navitar 12X Body Tubes, Rochester NY). As expected, partially filled electrodes showed a decrease in maximum actuation frequency and droplet motion speed, since only segments of the contact line are exposed to high electric fields.[6] Nevertheless, actuation frequencies of over 10 electrodes per second were achieved on devices with partially filled electrodes at a low electrode fill area of 40%, Fig. 3(b). This speed is sufficient for many biology and clinical applications of digital microfluidic devices.[14]

Removed areas on partially filled electrodes can be used for integrating other elements (e.g., heaters, detectors, and hydrophilic patches) into the electrodes; furthermore, they can be useful for on-chip imaging of droplet contents using transmission microscopy. Transmission microscopy imaging, particularly on inverted microscopes is a standard platform used in biology labs and clinics. Since completely filled, nontransparent electrodes made of metallic materials (e.g., Cr or gold) are not compatible with transmission microscopy imaging, ITO is typically used to construct electrodes.[4,10,15] However, ITO is more expensive in materials and fabrication than metallic electrodes, and the invisible ITO electrodes can pose challenges in device debugging. In comparison, partially filled metallic electrodes can be easier to construct while being compatible with transmission microscopy imaging.

Therefore, we intentionally constructed electrodes using metallic materials in this study to demonstrate their compatibility with standard transmission microscopy imaging. Partially filled Cr electrodes were used to actuate single mouse embryos. Morphology of the mouse embryos on

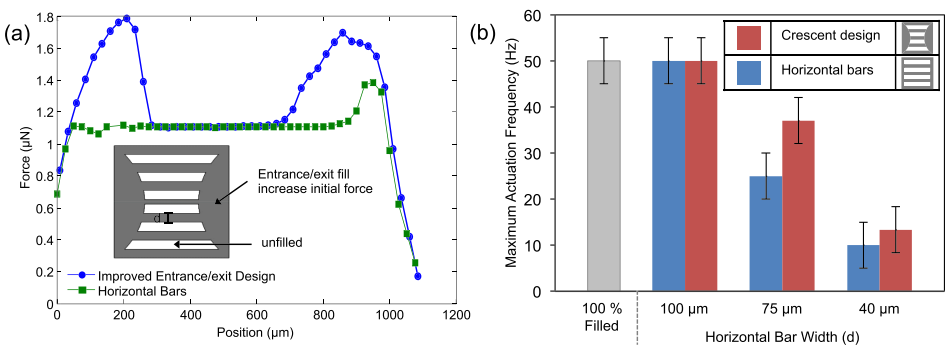

FIG. 3. (a) Simulation results: electrode design with crescent-like filled areas at the entrance and exit of the electrode produces increased force at beginning and end of droplet motion to create initial force to ensure droplet motion is generated. (b) Experimental comparison of electrode designs. In experiments, maximum droplet actuation frequency was measured at different fill percentages for normal and improved designs. Number of horizontal bars in the electrode was kept constant, thus reducing the bar width, reduces electrode fill percentage. Please note that reduction in maximum actuation frequency is almost proportional to the reduction in the bar width similar to the force reduction simulations. Experiments were conducted with deionized water at 75 V rms and 15 kHz by actuating droplet back and forth across a series of 5 electrodes at increasing speed until droplet motion could not keep up with actuation.

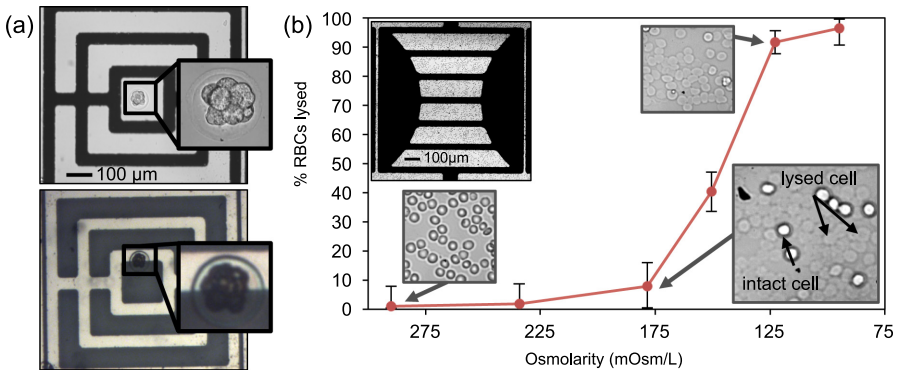

FIG. 4. (a) Single mouse embryo morphology on partially filled Cr electrodes. Upper image uses bright field transmission DIC imaging showing superior detail compared to reflection microscopy imaging used in lower image. (b) RBC viability measured with different osmolarities by counting cells through unfilled regions on chip. N = 150–600 for each osmolarity point.

partially filled electrodes was imaged under transmission differential interference contrast (DIC) microscopy, which revealed detailed embryo morphology and cell structures [Fig. 4(a)]. In applications, if the droplet medium is relatively viscous, the cell's position would remain relatively constant within the droplet. In this case, a set of partially filled electrodes negative of each other can be used to ensure that the cell can be imaged across these electrodes. If the cell's position does not remain constant with a less viscous droplet, the droplet can be easily actuated back and forth on partially filled electrodes until the cell rests on a non-filled region. Since it is viable to remove half of the electrode area without affecting generated forces significantly, a few actuations is typically sufficient to achieve cell imaging with this technique.

We also actuated droplets containing human red blood cells (RBCs) using partially filled Cr electrodes. Phosphate buffered saline (PBS) droplets containing RBCs were mixed with differing amounts of deionized (DI) water (i.e., varied osmolarity). RBC viability as a function of medium osmolarity was measured on chip. Lysed RBCs were easily identifiable on our partially filled electrodes under transmission microscopy, Fig. 4(b). The non-filled section on a single electrode was large enough to sample a significant portion of the population to gather meaningful statistics.

In summary, we investigated, numerically with preliminary experimental verification, the effect of removing sections of electrodes in digital microfluidic devices on the generated electrodynamic forces and the maximum achievable droplet speed. Generated electrodynamic forces were found to be linearly dependent on electrode fill percentage and independent of position of the horizontal non-filled areas. To maintain high initial pull for the droplet, we leave entrance and exit areas of the electrodes completely filled. As application examples, we constructed partially filled metallic electrodes and demonstrated their compatibility with standard transmission microscopy imaging. These results are meaningful for guiding the design of digital microfluidic devices that require the integration of other elements, such as detectors, heaters, and cell culture patches, on electrodes.

Y.S. acknowledges financial support from the Canada Research Chairs Program. M.A. acknowledges financial support from the Science and Technology development fund (STDF) through Grant No. 4081.

[1]S. K. Cho, H. Moon, and C. Kim, "Creating, transporting, cutting, and merging liquid droplets by electrowetting-based actuation for digital microfluidic circuits," J. Microelectromech. Syst. **12**(1), 70–80 (2003).
[2]M. G. Pollack and R. B. Fair, "Electrowetting-based actuation of liquid droplets for microfluidic applications," Appl. Phys. Lett. **77**(11), 1725–1726 (2000).
[3]I. Barbulovic-Nad, S. H. Au, and A. R. Wheeler, "A microfluidic platform for complete mammalian cell culture," Lab Chip **10**(12), 1536–1542 (2010).
[4]Y. Chang, G. Lee, F. Huang, Y. Chen, and J. Lin, "Integrated polymerase chain reaction chips utilizing digital microfluidics," Biomed. Microdevices **8**(3), 215–225 (2006).
[5]R. S. Sista, A. E. Eckhardt, V. Srinivasan, M. G. Pollack, S. Palanki, and V. K. Pamula, "Heterogeneous immunoassays using magnetic beads on a digital microfluidic platform," Lab Chip **8**(12), 2188–2196 (2008).
[6]M. Abdelgawad, P. Park, and A. R. Wheeler, "Optimization of device geometry in single-plate digital microfluidics," J. Appl. Phys. **105**(9), 094506 (2009).
[7]T. Lederer, S. Clara, B. Jakoby, and W. Hilber, "Integration of impedance spectroscopy sensors in a digital microfluidic platform," Microsyst. Technol. **18**(7–8), 1163–1180 (2012).
[8]S. K. Cho, Y. Zhao, and C. J. Kim, "Concentration and binary separation of micro particles for droplet-based digital microfluidics," Lab Chip **7**(4), 490–498 (2007).
[9]S. H. Au, S. C. C. Shih, and A. R. Wheeler, "Integrated microbioreactor for culture and analysis of bacteria, algae and yeast," Biomed. Microdevices **13**(1), 41–50 (2011).
[10]H. Ding, S. Sadeghi, G. J. Shah, S. Chen, P. Y. Keng, C. J. Kim, and R. M. van Dam, "Accurate dispensing of volatile reagents on demand for chemical reactions in EWOD chips," Lab Chip **12**(18), 3331–3340 (2012).
[11]K. Choi, J.-Y. Kim, J.-H. Ahn, J.-M. Choi, M. Im, and Y.-K. Choi, "Integration of field effect transistor-based biosensors with a digital microfluidic device for a lab-on-a-chip application," Lab Chip **12**(8), 1533–1539 (2012).
[12]D. Griffiths, *Introduction to Electrodynamics*, 3rd ed (Addison-Wesley, 1998).
[13]P. M. Young and K. Mohseni, J. Fluids Eng. **130**, 081603 (2008).
[14]R. B. Fair, A. Khlystov, T. D. Tailor, V. Ivanov, R. D. Evans, V. Srinivasan, V. K. Pamula, M. G. Pollack, P. B. Griffin, and J. Zhou, IEEE Design & Test of Computers **24**, 10 (2007).
[15]H. Kim, M. S. Bartsch, R. F. Renzi, J. He, J. L. Van de Vreugde, M. R. Claudnic, and K. D. Patel, "Automated digital microfluidic sample preparation for next-generation DNA sequencing," J. Lab. Autom. **16**(6), 405–414 (2011).